Anal. Chem. **2009,** *81,* 4183–4191

Articles

Fiber Optic Sensor for Simultaneous Determination of Atmospheric Nitrogen Dioxide, Ozone, and Relative Humidity

Shin-Ichi Ohira, Purnendu K. Dasgupta,* and Kevin A. Schug

Department of Chemistry and Biochemistry, The University of Texas at Arlington, 700 Planetarium Place, Arlington, Texas 76019-0065

We describe a novel optical sensor for the simultaneous measurement of atmospheric nitrogen dioxide (NO_2), ozone (O_3), and relative humidity (RH). A transparent backing thin layer silica gel chromatographic plate impregnated with 8-amino-1-naphthol-5-sulfonic acid (ANS) is used as the collection/sensor element. The plate transmittance is probed by three discrete light emitting diodes (LEDs) centered, respectively, at 442, 525, and 850 nm. The transmission of the plate changes reversibly across visible to NIR wavelengths as the RH around the plate changes; this is the basis for a limited-resolution RH sensor. The ANS on the plate reacts to form brown and pink colored products, respectively, when it reacts with NO_2 and O_3. The sample air impinges on the plate via an entrance nozzle. The LEDs are alternately turned on in a preprogrammed manner and the light is brought to the impregnated face of the plate by a three-legged fiber optic. The transmitted light is detected on the obverse side of the plate. The 850 nm signal provides the RH value and optionally serves as the reference measurement for the other two wavelengths; the NO_2 and O_3 reaction products do not absorb at this wavelength. The absorbance at 442 and 525 nm, thus referenced against 850 nm, are used to obtain NO_2 and O_3 concentrations from a pair of simultaneous equations. For a sampling period of 5 min, the limits of detection (LOD) based on 3 times the standard deviation of blank responses were 0.64 and 0.42 ppbv for NO_2 and O_3, respectively. Data obtained with collocated commercial instruments (O_3 induced chemiluminescence analyzer for NO_2 and UV-absorption for O_3) show good agreement. Overall, this provides a viable affordable approach for inexpensive measurement of atmospheric NO_2 and O_3.

Atmospheric nitrogen dioxide and ozone are among the six criteria air pollutants designated by the U.S. Environmental Protection Agency;[1] they are similarly classified in most other countries. National Ambient Air Quality Standards in the U.S. call for 53 parts per billion by volume (ppbv) or 100 $\mu g/m^3$ of NO_2 as the maximum annual arithmetic mean concentration and 75 ppbv of O_3 for a maximum 8 h average.[2] Much of the urban NO_x originates as nitric oxide (NO), but is largely converted to NO_2 by the reaction with O_3 in the atmosphere. On the other hand, NO_2 also generates O_3 via photochemical reactions in which reactive hydrocarbons are involved. In virtually all types of atmospheric models, NO_2 and O_3 are key parameters.[3−6]

Of many available methods for the measurement of atmospheric NO_2 and O_3,[7] the gas phase chemiluminescence reaction between NO and O_3 for the measurement of NOx[8] and the direct UV absorbance measurement for O_3[9] are the most commonly used. For the first case, the luminescence is

* To whom correspondence should be addressed. E-mail: dasgupta@uta.edu.

(1) The United States Environment Protection Agency. Six common air pollutants. http://www.epa.gov/air/urbanair/.
(2) The United States Environment Protection Agency. National Ambient Air Quality Standards (NAAQS). http://www.epa.gov/air/criteria.html.
(3) Uno, I.; Ohara, T.; Wakamatsu, S. *Atmos. Environ.* **1995**, *30*, 703–713.
(4) Shi, J. P.; Harrison, R. M. *Atmos. Environ.* **1997**, *31*, 4081–4094.
(5) Jang, J. C.; Jeferies, H. E.; Byun, D.; Pleim, J. E. *Atmos. Environ.* **1995**, *29*, 3085–3100.
(6) Padro, J.; Zhang, L; Massman, W. J. *Atmos. Environ.* **1998**, *32*, 1365–1375.
(7) NARSTO measurement methods compendium. http://narsto.orml.gov/compendium/methods.
(8) Fontijn, A.; Sabadell, A. J.; Ronco, R. *J. Anal. Chem.* **1970**, *42*, 575–579.
(9) Bowman, L. D.; Horak, F. A. Continuous Ultraviolet Absorption Ozone Photometer. In *Air Quality Instrumentation*; Scales, J. W., Ed.; Instrument Society of America: Pittsburgh, PA, 1972; Vol. 2.

10.1021/ac801756z CCC: $40.75
Published on Web 04/29/2009

weak; the instrument requires a cooled photo multiplier tube (PMT) sensitive to the near-IR. The measurement must be made at low pressures to avoid interferences from CO_2 and water vapor. In addition, NO_2 cannot be directly measured; it must first be reduced to NO. The absorbance-based O_3 monitor is more straightforward, based on the absorption of 254 nm light (typically supplied by a Hg lamp source) but a 2-channel differential measurement that involves selective destruction of O_3 is required. The response can also be humidity dependent.[10]

It is increasingly being realized that pollution, especially air pollution, is a global, rather than a local problem. While a wealth of monitoring data exists for developed countries, monitoring data are scarce for others. Perhaps even more importantly, without measurement there can be no factual knowledge on pollutant concentrations. Without such knowledge, public awareness cannot develop, and a popular will to mitigate the same remains elusive. Simple and affordable monitoring technologies are of paramount importance for developing countries in this context. In recent years we have made persistent efforts to develop simple sensors for O_3[11−14] and NO_2;[13,15,16] all of these depend on liquid phase reactions. To measure the entire amount of analyte collected in a small liquid volume so that the entire volume can be optically probed,[15] one has to rely on a chemiluminescence reaction[12] or probe the liquid volume in an efficient manner, as in a liquid core waveguide configuration.[11,13,14,16] Such liquid phase sensors have the limitation that a solution phase reagent creates for bulk and requires more frequent replacement. Further, reagents can often be unstable and colored products formed may deposit on system components creating for a gradually increasing system baseline. A liquid delivery means is also needed. A suitably impregnated solid collector has the advantages that it also integrates the analyte in a configuration that is easy to optically probe without involving exotic expensive low refractive index polymers. A reagent-impregnated solid collector has the disadvantage that the same area cannot be indefinitely used. This is not an insurmountable deterrent, filter tape samplers are in common use.[17−21] We show here a sensitive sensor based on a unique chemistry that responds sensitively to both NO_2 and O_3 and is reusable several times at typical ambient concentrations before a new area must be used.

EXPERIMENTAL SECTION

Reagents and Standard Gases. 8-Amino-1-naphthol-5-sulfonic acid (ANS, Sigma) was purified as follows. The reagent (1.5 g) was added to 450 mL of 0.1 M NaOH and gently warmed with stirring until most of the material dissolved. The very dark solution was filtered and 0.1 M HCl was added dropwise to the filtrate to first neutralize it and then adjust the pH to ~5. Off-white ANS crystals precipitate, are filtered off, and then recrystallized from hot water. ANS thus purified is nearly white.

Known concentrations of NO_2 in air were generated from gravimetrically calibrated permeation sources.[22] Ozone was generated with a pinhole aperture UV-lamp source and calibrated by standard iodometric methods.[23] Generation source and dilution air were supplied by a pure air generator (Model 737, AADCO, www.aadcoinst.com) and controlled by mass flow controllers (FC-280, Tylan General). Humidification to various degrees was controlled by bubbling an adjustable portion of the dilution air through a water bubbler while the humidity was monitored by a commercial sensor (225-HMP50YA, www.novalynx.com).

Impregnated Plates. After significant initial experimentation with various substrates, polyester backed thin layer chromatography (TLC) plates (250 μm thick, 60 Å pore silica gel, P/N 4410−221, Whatman) were chosen. These were cut into 25 × 25 mm squares. The impregnating solution was composed of 0.15% w/v purified ANS in phosphate buffer, the latter consisting of 13.78 g/L NaH_2PO_4 to which NaOH was dropwise added until pH 4 was reached. The squares were initially immersed into deionized (DI) water slowly from the edge; this removed water-soluble compounds from and also removed adherent air bubbles to allow uniform impregnation. The plates were then immersed into the impregnating solution for 15 min, removed, rinsed with DI water, kept in plastic chamber, and allowed to dry over 2−3 h under a gentle pure dry air flow stream. The prepared plates were kept in Ziploc bags in the dark at room temperature; they were stable in this condition easily for week-long periods.

Collection/Detection Cell. The structure of the sampler/detector is shown in Figure 1. The monitoring plate (MP) was placed, active side facing downward, between two opaque acrylic plates (top and bottom: TP and BP, 5 mm thickness), both containing a central aperture. A 1/4 in. tee provides the access through the bottom where three optical fibers (1.5 mm core, NT02-550, www.edmundoptics.com) were put into a 1/4 in. tubular stepped steel collar (affixed inside collar with epoxy) and inserted into the tee to illuminate the impregnated area. Air suction was provided through the tee arm by an air pump (AP, T2-01, www.parker.com). The sample air or zero gas entered via a 3-way solenoid valve (SV, 360T031, www.NResearch.com, Teflon wetted parts) for switching zero and sample gases. The sample air enters through a Teflon-lined stainless steel tube of 0.8 mm i.d. and impinges on the impregnated plate at an angle of ~45°. Zero air is supplied by passing the sample air through a purifier column consisting of a 60 mL disposable syringe filled with three successive layers of (from the entrance end) soda lime, charcoal, and silica gel. The sample gas flow rate was 0.4 standard liters per min (SLPM). The pump cannot provide this small flow rate in stable fashion; an adjustable make up flow through a ballast tube (BT) was therefore used. The free distal end of the three

(10) Wilson, K. L.; Birks, J. W. *Environ. Sci. Technol.* **2006**, *40*, 6361–6367.
(11) Dasgupta, P. K.; Genfa, Z.; Poruthoor, S. K.; Caldwell, S.; Dong, S.; Liu, S.-Y. *Anal. Chem.* **1998**, *70*, 4661–4669.
(12) Takayanagi, T.; Su, X.-L.; Dasgupta, P. K.; Martinelango, K.; Li, G.; Al-Horr, R. S.; Shaw, R. W. *Anal. Chem.* **2003**, *75*, 5916–5925.
(13) Toda, K.; Yoshioka, K.; Ohira, S.; Li, J.; Dasgupta, P. K. *Anal. Chem.* **2003**, *75*, 4050–4056.
(14) Li, J.; Li, Q.; Dyke, J. V.; Dasgupta, P. K. *Talanta* **2008**, *74*, 958–964.
(15) Cardoso, A.; Dasgupta, P. K. *Anal. Chem.* **1995**, *67*, 2562–2566.
(16) Milani, M. R.; Dasgupta, P. K. *Anal. Chim. Acta* **2001**, *431*, 169–180.
(17) Nakano, N.; Sugata, K.; Nagashima, K. *Anal. Chim. Acta* **1995**, *302*, 201–205.
(18) Nakano, N.; Yamamoto, A.; Kobayashi, Y.; Nagashima, K. *Bunseki Kagaku* **1993**, *42*, 537–541.
(19) Nakano, N.; Yamamoto, A.; Kobayashi, Y.; Nagashima, K. *Anal. Chim. Acta* **1999**, *398*, 305–310.
(20) Nakano, N.; Nagashima, K. *J. Environ. Monit.* **1999**, *1*, 255–258.
(21) Nakano, N. *Anal. Chim. Acta* **1996**, *321*, 41–45.
(22) Hughes, E. E.; Rook, H. L.; Deardorff, E. R.; Margeson, J. H.; Fuerst, R. G. *Anal. Chem.* **1977**, *49*, 1823–1829.
(23) Bergshoeff, G.; Lanting, R. W.; Prop, J. M. G.; Reynders, H. F. R. *Anal. Chem.* **1980**, *52*, 541–546.

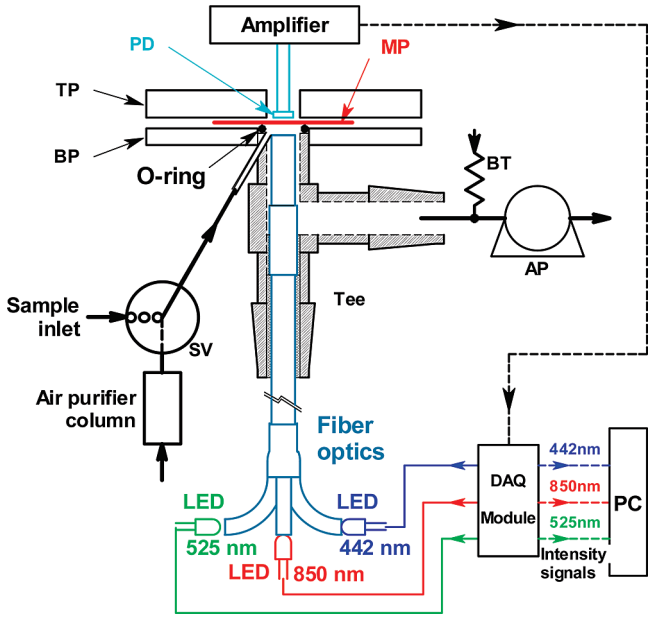

Figure 1. Schematic diagram of the detection system. LEDs were switched by the DAQ module and the light intensity of each LED was recorded separately. PD: photodiode; TP: top plate; BP: bottom plate; MP: monitoring plate; SV: solenoid valve; BT: ballast tube; AP: air pump.

optical fibers were respectively coupled to a λ_{max} 442 nm (L200-CWBK1KB-15D, 1 cd @ 20 mA www.ledtronics.com), λ_{max} 525 nm (NSPG500S, 11.6 cd @ 20 mA, www.nichia.com) and λ_{max} 850 nm (DN305, 10 mW @ 50 mA, www.stanley-components.com) LED. Light from the alternately switched LEDs pass through MP and is detected by the photodiode (PD, BPW34, www.vishay.com). To achieve comparable photodetector response, the LEDs were driven at 17, 15, and 10 mA, respectively. The LEDs were illuminated for 300 ms each and then all turned off for 100 ms; each was controlled via a N-channel logic level MOSFET switch (IRLI530N, www.irf.com) turned on by respective digital outputs from a notebook computer; this 1 s cycle was repeated indefinitely. The photocurrent was converted to voltage with 3.4 V/μA gain using a quad junction field effect transistor input operational amplifier (TL084CN, www.ti.com). The signal was acquired through a universal serial bus based data acquisition module of 14-bit resolution (USB-1014FS, www.measurementcomputing.com) on a personal computer using software written in-house. The software controlled LED illumination and separated the photodiode signal corresponding to each LED into different bins. The data were acquired at 100 Hz. For each 300 ms illumination period, the data for the central 100 ms illumination period was taken and averaged. The average dark period detector response was subtracted from each of these three separated LED transmittance signal averages and these values were recorded. At the beginning of a measurement cycle (vide infra) zero air is sampled, and the corresponding voltage signals are stored as I_0. After sample air is aspirated, the corresponding voltage signals are stored as I, and the absorbance values are thus computed as $\log I_0/I$. The measurement system sans notebook computer and data acquisition card was put into a plastic box ($20.5 \times 5.5 \times 15.5$ cm, $w \times h \times d$); Supporting Information, Figure S1 shows a photograph.

Atmospheric NO_2/O_3 Measurements. Atmospheric monitoring was performed by sampling air at an altitude of ~3 m above the roadbed of South Cooper Street (Texas State highway FM157), a busy 6-lane thoroughfare that bisects the urban Arlington campus of the University of Texas. The instruments were placed in a servicing room located in a bridge understructure and the sampling manifold was a 3.2 cm inner diameter PVC pipe (1.2 m long and lined with a polyester (Mylar) sheet to avoid sample gas adsorption) that reached out to the road through a ventilator grille. At the end of the pipe, a fan served to aspirate sample air from the outside with ~100 SLPM. The present system, an ozone chemiluminescence based NO-NO_x analyzer (Model 42, www.thermo.com) and UV-absorption based O_3 monitor (Model 202, www.twobtech.com), were connected to the manifold with short lengths of 1/4″ polytetrafluoroethylene (PTFE) tubes. The humidity sensor was directly inserted in the manifold. All of the instruments were calibrated with the same sources.

ANS-O_3 and ANS-NO_2 Product Structure Elucidation. A slight molar excess of NO_2 and O_3 were individually bubbled through respective 10 mL portions of a phosphate buffered 0.5 mM ANS solution. The characteristic colors of the reaction products in both cases were evident, and the product solution was subjected to chromatography−mass spectrometry. In both cases, chromatography showed that more than one product is formed while original unreacted ANS is also present. We focused our attention on the chromatographic peak that was the largest peak as monitored by 442 nm absorption in the NO_2 case and correspondingly the largest peak as monitored by 525 nm absorption in the O_3 case, as these are approximately the respective absorption maxima of the spectral absorption of the respective products observed on the plates. Thus, a photodiode array detector first monitored the chromatography effluent, and the effluent was thus accordingly sent to the mass spectrometer for further analysis. The instrumentation involved a Prominence high performance liquid chromatograph with photodiode array detector (HPLC-PDA) coupled online to an electrospray ionization-ion trap-time-of-flight (ESI-IT-TOF) mass spectrometer. Both NO_2 and O_3 reaction product solutions (nominally 500 μM) and unreacted ANS (250 μM) samples were injected onto a Shimpack XR-ODS C18 column (2.0 × 75 mm, 2.2 μm d_p (all above from www.Shimadzu.com). The gradient program was 92% A (20 mM aqueous CH_3COONH_4), 8% B (acetonitrile) held isocratic for the first 6 min then linearly ramped to 2% A, 98% B in 6 min and then held for 3 min, followed by a re-equilibration at 8% B for 6 min; the flow rate was 0.2 mL/min. The ESI-IT-TOF data in the negative ionization mode only are discussed here; multiple mass analysis events were used to collect tandem mass spectrometry data up to MS^3 (50−800 m/z scan range) for the peaks selected on the basis of the PDA response. Time-of-flight detection was externally calibrated using sodium trifluoroacetate providing less than 5 ppm error in mass accuracy. Formula Predictor software (Shimadzu) was used to produce elemental formulas for each of the reaction products, utilizing both high mass accuracy full scan and tandem mass spectrometry data, as well as observed isotopic abundances.

RESULTS AND DISCUSSION

Impregnated Solid Sensor and Choice of Optical Interrogation Modes. Different impregnated filter tapes have been used to monitor various gases;[17−20] the use of reagent impregnated porous glass [24,25] has also been reported. Of note is the use of Griess−Saltzman (G-S) reagent for monitoring NO_2.[21] The sample gas is generally drawn through the porous filter tape. There is one report where the gas is not drawn through the filter but the gas impinges on the filter that is impregnated with silica gel to increase reagent impregnation capacity.[26] We reasoned that if the reagent holding capacity is high we can use the same reagent impregnated area either several times over short discrete measurement intervals or over a long period before the reagent is exhausted and the response saturates. It is also necessary to probe all of the collected/reacted material optically. This cannot be done by reflectance measurements which are nearly universally used with impregnated solid sensor monitoring. Reflectance primarily probes the surface layer, and reflectance data generally need some form of transformation prior to relating them to concentration.[27,28] Transmittance measurement in contrast probes the entire reacted/collected mass. We also reasoned that using highly porous small silica particles in a loosely packed thin layer form will provide the best opportunity to use the impregnated region most effectively. Thin layer chromatography (TLC) plates with a 250 μm layer silica gel 60 (60 Å pores) in fine size (2−25 μm dia.) meet these criteria; since these plates are available with transparent plastic backing, probing in the transmission mode is simple. We actually also found that at least with our present set up, more light was transmitted than reflected; the reflection mode had a 5.2× larger noise than the transmission mode.

Colorimetric Chemistry and Initial Test Results. Despite the fact that the chemistry has a known interference from ozone,[29] by far the most widely used colorimetric technique for NO_2 measurement involves the G-S reagent. The reaction is sensitive but slow at room temperature and requires relatively strongly acidic conditions; however, the solubility of NO_2 into a solution decreases with decreasing pH.[30] Nakano[21] achieved the acidity by incorporating *p*-toluenesulfonic acid in the reaction mixture. There is virtually no reaction when the reaction surface is dry; large amounts of glycerin in the impregnating reagent were used by Nakano. Unfortunately this did not eliminate humidity dependence: at low humidities the response decreased with increasing sample flow rate while at high sample humidities precisely the opposite occurred. The concentration versus response exhibited two distinctly different linear regions with a drastic change in slope.[21] With a sampling interval of 10 min, the best LOD that could be attained was 1 ppbv. Our initial experiments with G-S reagents were also disappointing; the response was too slow. We decided to explore ANS that the senior author discovered early on[31] to be an interesting reagent that in solution diazotized at a modestly acidic pH and then coupled to itself forming a brown product, all much faster than the G-S reaction, albeit the sensitivity was much less than that obtained with the G-S reagent.

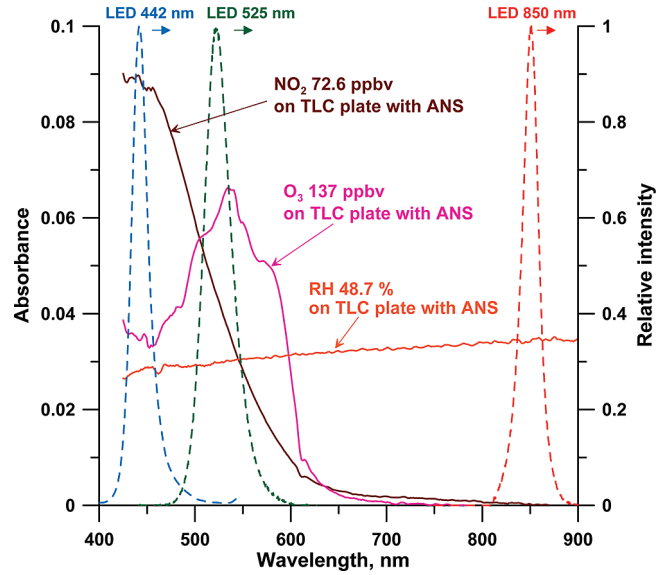

Figure 2. Spectra of the products of reaction of an ANS-impregnated plate respectively exposed to 72.6 ppbv NO_2, 137 ppbv O_3 and humid air (48.7% RH) for 5 min obtained with a 20 W tungsten light source (www.optometrics.com) and a fiber-optic spectrometer (CDI-PDA/280−1000/1.5/25 μm, www.controldevelopment.com). For the LEDs used in this work, the light intensities as a function of wavelength (normalized to unity1 at λ_{max}) are also shown.

Initial tests with this reagent were encouraging. We planned on pairing ANS with indigotrisulfonate that is selectively bleached by ozone[13,14,32] either in the same formulation or as a separate adjacent spot to make a combined NO_2/O_3 sensor. Before testing such a combined reagent, we elected to conduct a preliminary ambient air test alongside a commercial NO_2 monitor. The results were disappointing: the colorimetric sensor consistently read higher than the chemiluminescence based NO_2 monitor. Visually the exposed plates also showed a distinctly different hue from what we observed with the NO_2 exposed plates in the laboratory. To investigate what is causing this interference, we reacted ANS in solution either with solution phase reagents or by bubbling gases. Carbon dioxide/bicarbonate, sulfur dioxide/bisulfite, nitric acid/nitrate, ammonia, and sulfide showed no color change. But to our considerable surprise, the solution turned bright pink when ozone was bubbled through it; we had expected at best bleaching of any extant color that most commonly happens with ozone. We exposed plates individually to NO_2 and O_3 and the resulting transmission spectra of the exposed plates, obtained with a white light source and a fiber optic spectrometer are shown in Figure 2. While the spectra do overlap they also differ. By making measurements at two (or more) wavelengths, it should be possible to simultaneously assess NO_2 and O_3 concentrations. We chose LEDs with emissions centered at 442 and 525 nm; the emission spectra

(24) Tanaka, T.; Ohyama, T.; Yamada Maruo, Y.; Hayashi, T. *Sens. Actuators B.* **1998**, *47*, 65–69.
(25) Tanaka, T.; Guilleux, A.; Ohyama, T.; Hayashi, T. *Sens. Actuators B* **1999**, *56*, 247–253.
(26) Suzuki, Y.; Nakano, N.; Suzuki, K. *Environ. Sci. Technol.* **2003**, *37*, 5695–5700.
(27) Ragain, J. C.; Johnston, W. M. *J. Dent. Res.* **2001**, *80*, 449–452.
(28) Plieth, W. J.; Naegele, K. *Surf. Sci.* **1975**, *50*, 53–63.
(29) Baumgardner, R. E.; Clark, T. A.; Hodgeson, J. A.; Stevens, R. K. *Anal. Chem.* **1975**, *47*, 515–521.
(30) Toda, K.; Hato, Y.; Mori, K.; Ohira, S.; Namihira, T. *Talanta* **2007**, *71*, 1652–1660.
(31) Dasgupta, P. K. *Anal. Lett.* **1984**, *17*, 1005–1008.
(32) Darby, J. L.; Chang, D. P. Y.; Coggin, P. S.; Chung, H. K.; Dasgupta, P. K. *Process Control Qual.* **1995**, *6*, 229–243.

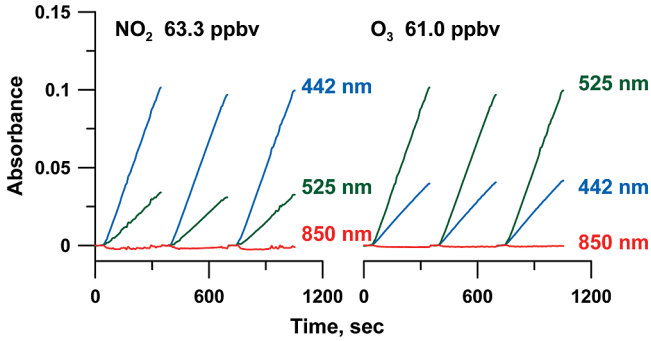

Figure 3. Typical response of the system to dry individual test gases (0.4 SLPM sample flow). Note that in each case the response linearly increases with time. The slope of each line is proportional to the gas concentration.

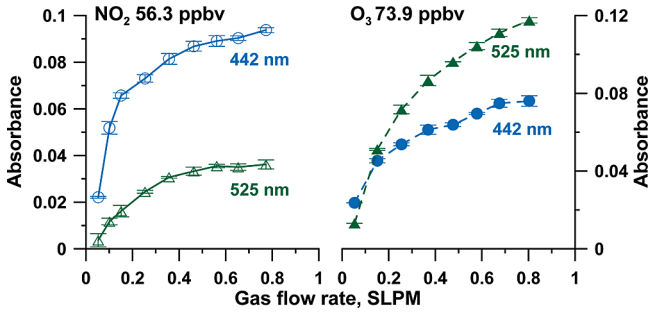

Figure 4. Effects of the gas flow rate on the response. Results for 56.3 ppbv NO_2 and 73.9 ppbv O_3 are shown. Circles and triangles depict the response at 442 and 525 nm, respectively.

for these LEDs are also shown in Figure 2. Particularly for the later LED, based on the spectral data shown in Figure 2, any wavelength between 525 and 600 nm would have been acceptable.

Typical response of the system and ANS reagents for NO_2 and O_3 are shown in Figure 3. It can be seen that absorbance, both at 442 and 525 nm, increase linearly with time with either gas.

Parametric Effects. *Sample Flow Rate.* Figure 4 shows the effect of the gas flow rate on the response for 56.3 ppbv NO_2 and 73.9 ppbv O_3. The absorbance values shown are from a sampling time of 5 min. The response increased monotonically with flow rate. But only at low flow rates did the response increase linearly with the flow rate. It is obvious that the overall response dependence on flow rate will depend on the exposed plate area, the exit velocity of the gas from the entrance tube (and hence tube diameter), and the precise position of the nozzle with respect to the center of the plate (in the present instance, 0.5 mm). None of these parameters were optimized. As the flow rate increases, a lower fraction of the entering analyte molecules will see the plate, and it will be expected that the d(absorbance))/d(flow rate) slope will decrease with increasing flow rate. It is interesting to note that as the flow rate increases, the visible diameter of the spot size after exposure also increases. Since our absorbance measurements are not spatially discriminating, it is not possible to judge whether the increased flow effectively causes a greater area to be exposed or the greater mass influx simply makes a greater area visible. To get good response sensitivity, we arbitrarily chose a sample flow rate of 0.4 SLPM. At this flow rate the visible spot size after 5 min sampling at the stated concentrations, which are typical of high ambient urban concentrations, was 3.5 mm, slightly larger than the photodiode active area (~3 mm). In reality, for urban sampling where the system detection limit is not an issue, it would be better to choose a lower sampling rate to allow longer usable lifetime of the same exposed area.

Individual Calibration Behavior. Individual calibration for both gases was conducted (0−120 ppbv NO_2, 0−125 ppbv O_3) with ΔA measured for a 5 min sample period with 0.4 SLPM sample flow. For both gases at both wavelengths, the absorbance responses were linear (r^2 ranged from 0.9933−0.9980), calibration data are shown in detail in Supporting Information, Figures S2 and S3. The LODs based on individual exposures with 3 times the standard deviation of zero air were 0.68 and 1.40 ppbv for NO_2 at 442 and 525 nm, respectively. The corresponding LODs for O_3 were 1.74 and 0.69 ppbv at 442 and 525 nm, respectively. This suggests a linear dynamic range of 2 orders of magnitude. We have not conducted thorough calibrations at concentrations above the stated range, but individual measurements at 200 ppbv suggest that the response decreases relative to extrapolations from lower values. A quadratic calibration equation can be used but an obvious appropriate measure is to reduce the sampling rate and/or exposure duration.

Simultaneous Determinations. Simultaneous determination of two analytes is commonly practiced with the same chemistry, with some external parameter to bring about differentiation. Fluorescein mercuric acetate reacts with both H_2S and CH_3SH and differentiation can be achieved by a collector that collects both gases in conjunction with a collector that collects only H_2S.[33] Similarly both As(III) and As(V) can be reduced to form arsine, but the reduction conditions can be used to control whether both or only As(III) is reduced.[34,35] The present situation is different: the same reagent leads to different products with the two analytes that absorb differently, akin to the formation of a red and blue product, respectively, with mercaptans and sulfide from Emil Fischer's reaction.[36] However, the spectral overlap in that case at the chosen monitoring wavelengths was small; in the present case the NO_2 reaction product absorbs 3 times as strongly at 442 nm as it does at 525 nm, whereas the O_3 reaction product absorbed 1.75 times more intensely at 525 nm relative to 442 nm. A white light source and a full spectrum detector as used in Figure 2 would have obviously improved limits of detection, and so on, but our primary objective was to build a monitoring system for developing countries at as low a cost as possible.

On the basis of calibration data with various mixtures containing 0−120 ppbv NO_2 and 0−125 ppbv O_3, we developed the quantitation equations.

$$NO_2, \text{ppbv} = 0.752A_{442} - 0.428A_{525} \quad (1)$$

$$O_3, \text{ppbv} = 1.14A_{525} - 0.380A_{442} \quad (2)$$

(33) Toda, K.; Ohira, S.; Tanaka, T.; Nishimura, T.; Dasgupta, P. K. *Environ. Sci. Technol.* **2004**, *38*, 1529–1536.
(34) Toda, K.; Ohba, T.; Takaki, M.; Karthikeyan, S.; Hirata, S.; Dasgupta, P. K. *Anal. Chem.* **2005**, *77*, 4765–4773.
(35) Idowu, A. D.; Dasgupta, P. K.; Genfa, Z.; Toda, K.; Garbarino, J. R. *Anal. Chem.* **2006**, *78*, 7088–7097.
(36) Lei, W.; Dasgupta, P. K. *Anal. Chim. Acta* **1989**, *226*, 165–170.

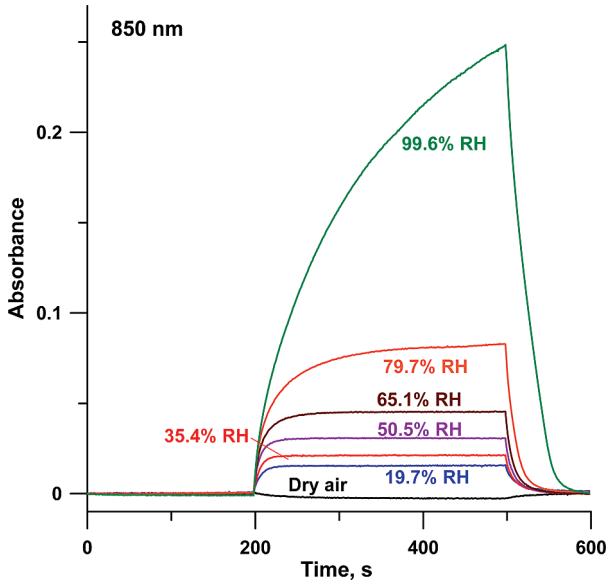

Figure 5. Plate is exposed to test clean air containing variable humidities between 200 and 500 s and is exposed to dry zero air at other times. The measured absorbance of the plate increases with increasing humidities very similarly at all wavelengths, the data for 442 and 525 nm are shown in Supporting Information, Figures S4 and S5.

We chose not to pursue a response model that included an NO_2-O_3 interactive term, as eqs 1 and 2 predicted the known (non-zero) analyte concentrations within ±3% for the mixture of 20/40 and 40/80 ppbv NO_2/O_3 mixtures. Similarly we tested a mixture of 15.6/56 ppbv NO_2/O_3, where the proportion of O_3 is higher; the same standard equations predicted 12.1 ± 2.1 and 50.7 ± 0.87 ppbv NO_2 and O_3, respectively.

Effects of Relative Humidity. Humidity can affect uptake of the test gases and affect the rate or extent of the reaction itself. For example, the G-S reagent hardly reacts with NO_2 at low humidities in the absence of a humectant to retain moisture.[21] At the outset, we observed a yet unanticipated effect: the transmittance of the silica plate decreased with increasing humidity, first slowly and then more significantly at higher humidities. Note that this is exactly opposite to the plate being wetted by liquid water; the transmittance is higher for a wetted plate. The change in absorbance as a function of RH is seen throughout the VIS−NIR range; however, as can be seen for the absorption spectrum for a plate exposed to clean air at 48.7% RH in Figure 2, the absorbance increases in a very minor fashion with increasing wavelength. The change in absorbance with increasing RH is also nearly invariant with wavelength. As ANS and its reaction products do not significantly absorb at 850 nm and high intensity emitters are available at this wavelength, we chose to probe the effect of RH at this wavelength. Figure 5 shows this temporal change in light transmission at 850 nm during a 5 min exposure to clean air of differing humidities. It will be observed that the response time increases with increasing sample humidity; however, at all but very high humidities, equilibrium response is attained within a few minutes, and this can form the basis for a simple humidity sensor. The decrease in transmittance with increasing sample humidity is observed at all wavelengths; the data comparable to that in Figure 5 are shown in Supporting Information, Figures S4 and S5 for 442 and 525 nm, respectively.

The change in light transmittance as a function of humidity, however, requires that analyte data be corrected for it. Fortunately, the transmittance ratio of the blue or green LEDs with respect to the 850 nm LED remains virtually constant except at the highest, near saturation humidity tested. Figure 6a shows the transmittance ratios during the final 200 s of a 300 s exposure period for a 19.7% RH exposure and a 99.6% RH exposure. This ratio remains essentially constant during the exposure with the exception of the blue/NIR ratio for the near-saturation humidity exposure. All other exposures also show a constant ratio; the blue/NIR ratio for the 79.7% RH exposure is shown as an additional example. Figure 6b shows the transmission ratio at the end of 5 min of exposure and how the transmittance at 850 nm changes as a function of RH. This behavior provides several options to correct for humidity dependence of the plate transmittance:

(a) The green and blue LED signals can be referenced to the 850 nm signal; this will result in negligible error for humidities up to 80% RH and ~ ±7% error at saturation humidity. Also, at humidities higher than 80% RH, the exact humidity can be measured by the 850 nm signal and individual transmission correction factors for the transmission ratios can be applied to the blue and green LED signals without assuming they are unity.

There are also options that do not involve the incorporation of an 850 nm light source:

(b) As shown in Figure 5, the humidity effect is reversible, switching back to dry air for as little as 90 s will completely reverse the humidity effects on the plate. The results with this option are shown in Figure 7 and will result in error bounds of ~±4%.

(c) Because it is possible to use the plate repeatedly (vide infra) and relative humidity does not generally change markedly within a 5 min measurement interval, the delta absorbance at any wavelength over 5 min is not expected to be markedly affected by humidity because there cannot be any marked humidity change.

However, these approaches cannot compensate for any changes in uptake and reactivity as a function of humidity. Supporting Information, Figures S8 and S9 show that statistically there is no consistent effect of humidity on the intrinsic response of this chemical sensor to the analytes of interest.

Reproducibilty of Plates. The reproducibility of the plates was tested both with respect to preparation and response. Each plate was measured (by NaOH extraction and fluorometric determination of ANS, see Supporting Information for details) to contain 42 ± 7 nmol ANS/cm^2, amounting to 13 ± 2 nmol ANS for the exposed/probed area. Each of four plates was tested by exposure to 21.3 ppbv standard NO_2 gas in four different areas of the plate. The standard deviation of response from different areas ($n = 4$) on the same plate ranged from 1.2 to 4.7% from plate to plate ($n = 4$), and the variance of all of the measurements comprising the different areas of all the plates amounted to 4.4%.

Capture Efficiency, Sensor Capacity, and Reusability. It can be inferred a priori that high velocity gas flow impinging on a solid substrate provides very little contact time, and some of the gas molecules may not even contact the substrate, thus limiting capture efficiency. To determine the fraction of the gas captured, we measured the gas concentration before and after the device with a commercial analyzer. This experiment can only

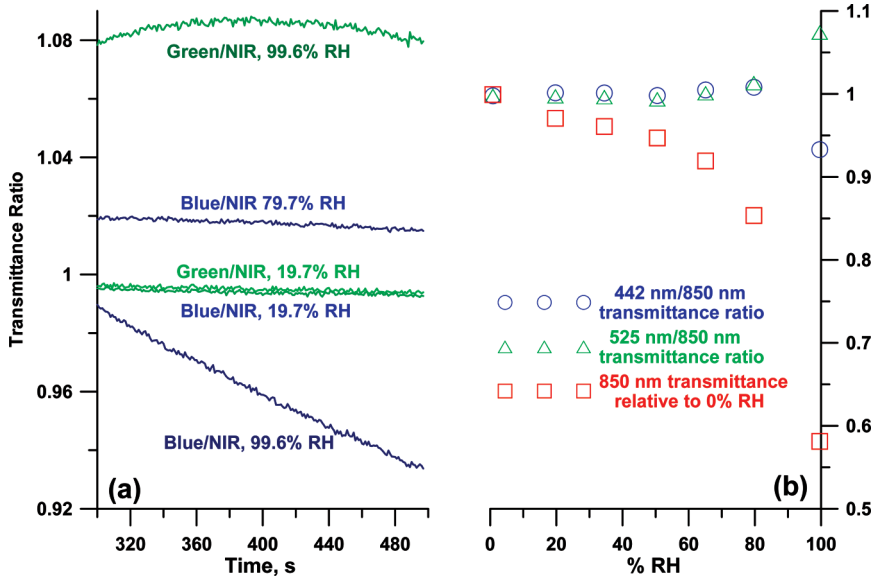

Figure 6. Transmittance ratios. (a) Continuously for the 300−500 s period (see Figure 3) during exposure to sample air and (b) the final transmittance ratio of blue/NIR and green/NIR LEDs after 5 min of sampling.

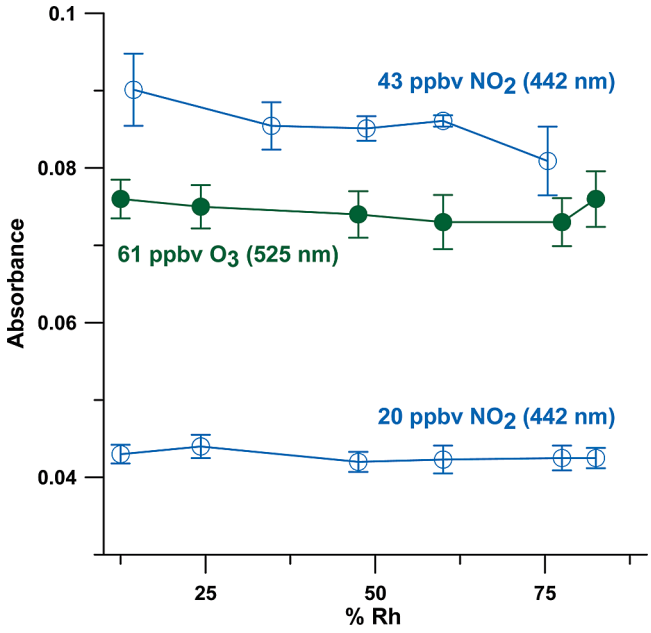

Figure 7. Effect of humidity on amount of product formed. Following sampling, dry zero air was sampled for 5 min to remove moisture prior to reading data.

be unambiguously carried out in the NO_2 case, whereas ozone decomposition can occur without reactive chromogenic capture. A NO_2 standard gas (170 ppbv) was admitted into the sensor at 0.4 L/min; a ballast pure air flowstream was added to meet the flow demands of the CL-based NO_x analyzer. The exit gas concentration was measured with and without the impregnated plate. For the initial 5 min exposure, 18.5 ± 0.1% of the NO_2 was captured, but the sensor gradually saturated and by 30 min the overall capture dropped to nearly half this value (9.10 ± 0.03%, $n = 2$). Accordingly, the sensor response is initially linear and then gradually the slope decreases. As may be expected, sensor saturation depends on the exposure dose and not the concentration. The acceptable upper limit will obviously vary depending on the criteria put on by the user. An exposure dose of 1 ppm s can be considered to be a rather modest value (corresponding to a concentration of 3.3 ppbv NO_2 for 5 min or see Supporting Information, Figure S2 for the results of exposure to 20.9 ppbv for ~50 s), as Figures S2 and S3 in Supporting Information show, the same linear response is maintained to an exposure dose of 3.6 ppm s (119 ppbv for 300 s). Exposure to 170 ppbv NO_2 over longer periods further show that in terms of response/unit exposure dose, there is <5% change from the initial response to 1 ppm s up to an exposure dose of ~45 ppm s. To put matters in perspective, here in Arlington, TX, an urban area, the average concentration of NO_2 during the 2005−2007 period was 11 ppbv.[37] At this concentration, the same spot can be reused about 13 times with <5% error. If the stringency is relaxed, the upper exposure limit will be greater. For example, up to 184 ppm s exposure dose, the relationship between exposure dose and A_{442} exhibited a linear r^2 value ≥0.95. Finally, computational costs continue to decrease. On the basis of each measurement that has just been made and the exposure ascertained, the response factor for the next exposure can be based on the prior dosage the sensor has already received. We illustrate this for the NO_2 exposure case in Figure S6 in Supporting Information as to how a new response factor can be chosen based on the prior exposure history. The caveat is not to overextend this approach—we use as a practical limit a point where the incremental response is half the initial value. In addition, exposure doses for both O_3 and NO_2 must be considered together.

Reaction Chemistry. In terms of products formed, we have tried here only to decipher the identity of dominant product(s), as chromatography clearly shows that more than one product is formed in both NO_2 and O_3 cases, at least under preparative conditions. For NO_2, in keeping with the well-known chemistry of the Griess−Saltzman reaction, it was previously[31] suggested that the amine group is diazotized and the diazonium cation

(37) Texas Commission on Environmental Quality. CAMS 61 Nitrogen Dioxide Summary. http://www.tceq.state.tx.us/cgi-bin/compliance/monops/yearly_summary.pl.
(38) Linnert, K. *Clin. Chem.* **1999**, *45*, 314–315.

then couples to a second molecule of the ANS, likely in the 4- or 2- position (*p*- or *o*- to the -OH group) or both. On a solid substrate, mobility of the diazonium cation formed will obviously be limited and reaction with a second molecule may be difficult. In the present case, all the ANS reaction products, in either the NO_2 or the O_3 reaction case, provide much stronger signal intensities in the negative ion mode than in the positive ion mode. This is consistent with the sulfonic acid moiety being intact and that strongly acidic proton readily coming off. As such, in a moiety in which the diazonium group is present as the cation and the -SO_3H group has lost a proton, overall the species will have no net charge and will not be detected by the MS.

We studied the chromatographic peak of pure ANS by subjecting it to the same type of analysis conducted with the product peaks. The measured mononegative $[M-H]^-$ ion parent mass at 238.0182 Th (1 Thomson (Th) = 1 m/z unit, see ref 39) was correctly interpreted by the formula predictor software which predicted an elemental formula (EF) of $C_{10}H_9NO_4S$; (theoretically 238.0180 Th for the $[M-H]^-$ ion; this represents a 0.84 ppm error, well within the calibrated accuracy of ±5 ppm for the instrument).[40] The software also reports an "Iso score" based on the isotopic analysis fragments generated by MS^n; the higher the Iso score, the greater is the confidence that the EF has been correctly predicted. For this reference case of ANS, the Iso score was reported to be 36.60. Tandem mass spectra recorded for ANS and the dominant product ions described below can be found in the Supporting Information.

For the major NO_2 reaction product eluting at ~9.8 min, the dominant parent molecular ion was at 311.9924 Th. The most likely EF was predicted to be $C_{10}H_7N_3O_7S$ (theoretical: 311.9932 Th for the $[M-H]^-$ ion; −2.56 ppm error, again well within the calibration accuracy) with an excellent Iso score of 64.95. This indicates the loss of two H atoms and the gain of two N and three O atoms. Previous work[31] showed that the diazotization is fast and the diazonium cation has a broad absorption (in solution) centered at ~450 nm, whereas the diazo coupling product forms slower and has a broad absorption centered at ~550 nm. Chemically it is therefore logical that the product we are looking at is the diazonium salt in the nitrate form, that is, the product is 1-naphthol-5-sulfonato-8-diazonium nitrate. It is known from previous work that reactions of Calix[4]arenes with NO_2 similarly results in the formation of Calix[4]arenenitrosonium nitrate.[41,42]

For the observed O_3 reaction products, the dominant peak absorbing at 525 nm eluted at ~9.3 min and generated a mononegative parent ion signal at 254.0119 Th. The most probable assigned EF was $C_{10}H_9NO_5S$ (theoretically 254.0129 Th for the $[M-H]^-$ ion; this represents a −3.94 ppm deviation) with an Iso score of 52.18. This merely represents the addition of one O atom to ANS. The oxidation of phenols by ozone has been studied in the past; such studies have generally been conducted with a sizable excess of ozone and generally the major pathway is ring-opening and eventually complete destruction of the skeleton. However, even in these cases, formation of *p*-quinones has been noted.[43] In the present case, where a limited amount of analyte must contact an excess of reagent, any formation of a quinone must proceed via the hydroquinone. The above EF corresponds exactly to the hydroquinone where an additional hydroxyl group is introduced in the 4-position, that is, to form 8-amino-5-sulfonato-1,4-naphthalene-diol. We propose that this is the primary ozone oxidation product (Supporting Information, Scheme 1).

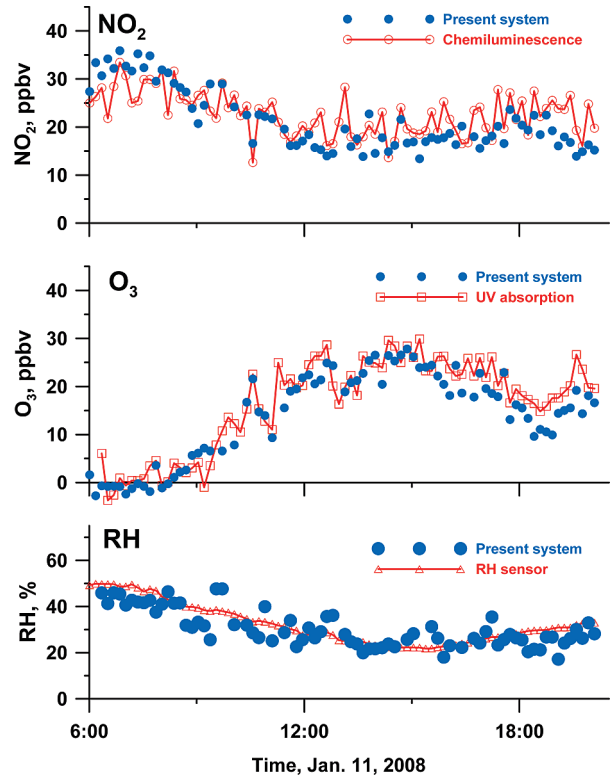

Figure 8. Comparative ambient air measurement data with present system against standard benchmark instrumentation.

Application to Ambient Air Analysis. The present system was applied to the analysis of ambient air and compared to data generated by benchmark instrumentation. The present results were obtained for 5 min samples, and the results obtained with the commercial detectors were averaged over the same period. The results are shown in Figure 8 for 1 day of sampling. The pattern is typical of many urban areas. The concentration of NO_2 starts high in the morning. The concentration of ozone increases after the morning traffic hours as insolation intensity increases and $[NO_2]$ decreases concurrently. Ozone concentration does not begin to decrease until after mid-afternoon with the decrease in solar flux.

The average (±sd) concentrations were 21.4 ± 6.4 and 14.1 ± 9.3 ppbv for NO_2 and O_3, respectively. The regression plots and difference plots[38] between the present and the benchmark detectors are shown in Supporting Information, Figure S7. The slopes of the correlations were 0.94 and 0.88 for NO_2 and O_3, respectively. Note that the present system was continuously sampling for 5 min intervals, and the strip was

(39) Cooks, R. G.; Rockwood, A. L. *Rapid Comm. Mass Spec.* **1991**, *5*, 93.
(40) Bristow, A. W. T. *Mass Spectrom. Rev.* **2006**, *25*, 99–111.
(41) Zyryanov, G. V.; Kang, Y.; Rudkevich, D. M. *J. Am. Chem. Soc.* **2003**, *125*, 2997–3007.
(42) Ohira, S.-I.; Wanigasekara, E.; Rudkevich, D. M.; Dasgupta, P. K. *Talanta* [Online early access]. DOI: 10.1016/j.talanta.2008.10.024. Published Online: **2008**; in press.
(43) Razumovskii, S. D.; Ovechkin, V. S.; Konstantinova, M. L. *Russ. Chem. Bull.* **1979**, *28*, 261–264.

semimanually advanced. The commercial instruments were switching zero and sampling mode with 10 and 5 s intervals for NO_2 and O_3, respectively. The O_3 concentration with the present system was ~12% lower on average than the values reported by the UV-absorbance system. The present UV-based O_3 monitor did not include a Nafion dryer that had been incorporated into later generations of this monitor to eliminate humidity effects, and in part the difference may be due to this cause;[10] all calibrations were conducted with dry O_3, as is customary. The difference plots indicate no apparent bias as a function of concentration.

In summary, we have demonstrated a very affordable solid phase gas collector/detector that can simultaneously measure NO_2, O_3, and RH with 5 min time resolution (the RH sensor actually responds much faster). Commercial systems with the same LOD and applicable range can offer much better time resolution, but three separate instruments are needed with considerably greater cost, size, and weight. Commercial CL-based NO_2 analyzers must actually switch between NO_x and NO to obtain NO_2 by difference and require substantial power. The present system can be battery powered, can operate without warm up time, and is thus ideally suited for spot checking concentrations in the field without requiring compressed gases. The principle can be adapted to filter-tape monitors. We hope to report on a disk shaped sampler that takes advantage of stepper motor drives inexpensively incorporated into portable CD players (Supporting Information, Figure S10) in the near future.

ACKNOWLEDGMENT

This work was supported in part through U.S. EPA Science To Achieve Results (STAR) Program Grant RD-83107401-0 and in part by the National Science Foundation through Grant CHE-0731792. We thank Jeff L. Johnson, Facilities Management, The University of Texas at Arlington, for facilitating collocated measurements at the Cooper Street site.

SUPPORTING INFORMATION AVAILABLE

Additional information as noted in the text. This material is available free of charge via the Internet at http://pubs.acs.org.

Received for review August 21, 2008. Accepted April 15, 2009.

AC801756Z